JOURNAL OF MATERIALS SCIENCE 30 (1995) 1173–1179

Mechanical properties of monolithic AlN and SiC_w/AlN composites

C. K. UNNI
M and J Technologies, Odessa, Texas, USA
D. E. GORDON
Lockheed, Fort Worth Company, Fort Worth, Texas, USA

Flexural, tensile, and high cycle fatigue test data are presented for pressureless sintered aluminium nitride (AlN) and hot-pressed aluminium nitride reinforced with silicon carbide whiskers (SiC_w/AlN). Tests were conducted at ambient temperature. The SiC_w/AlN composites consisting of 30 wt% SiC_w produced significant increases in flexural strength, tensile strength, and tensile fatigue strength compared to monolithic AlN. Increases were nearly double in all cases. Corresponding strain-to-failures measured in tensile tests increased from $\sim 0.04\%$ in monolithic AlN to $\sim 0.10\%$ in the SiC_w reinforced composite. Fracture surfaces showed evidence of whisker-toughening mechanisms due to additions of SiC_w whiskers. High-cycle fatigue results indicated that both materials have the ability to sustain higher stress levels in the cyclic tests compared to the tensile experiments. The improved performance under cyclic testing is explained in terms of strain-rate effects. The times at or near peak stress are considerably less under high-cycle fatigue testing (20 Hz) compared to tensile tests (strain rate = $0.5\%\,min^{-1}$).

1. Introduction

Structural ceramics have received considerable attention in recent years for high-temperature applications. These applications include (1) hypersonic vehicles and (2) energy-conservation devices. Increased efficiency, derived from higher operating temperatures, has been the incentive of the development of these high-temperature ceramics. Besides high-temperature strength capabilities, other advantages of these ceramic materials are oxidation and corrosion resistance, low bulk density, excellent creep and wear resistance and potential lower cost.

Despite this effort, however, large-scale application of structural ceramics in critical components has not occurred. The principal reason is the low toughness of ceramics, which makes them prone to catastrophic failure, thus raising reliability concerns. SiC whisker reinforcement of ceramics can result in substantial improvements in fracture toughness and resistance to wear, slow crack growth, and thermal shock of ceramics with the incorporation of strong, small diameter ceramic whiskers [1–5]. For example, the critical toughness of very fine-grained alumina can be increased from $\leqslant 3\ MPa\,m^{1/2}$ to $9\ MPa\,m^{1/2}$ with the addition of 20 vol% SiC whiskers. Comparable increases in toughness have been observed in a variety of other whisker-reinforced ceramics [3, 4]. The mechanisms responsible for such whisker toughening include crack deflection and both whisker bridging and whisker pullout within a zone immediately behind the crack tip [1–5]. Such processes have been noted in fracture-surface observations and scanning and transmission electron microscopy studies of cracks in these composites. The increased fracture toughness of whisker-reinforced ceramics can be retained with increasing temperature, e.g. up to about 1100 °C in the SiC whisker-reinforced alumina composites [6]. When compared with the continuous fibre-reinforced ceramics at the same reinforcing phase contents, the whisker-reinforced composites exhibit similar toughness values, but have the advantage of composite fabrication by more conventional powder processing techniques.

Aluminium nitride ceramic prepared at high temperature has drawn great attention, owing to its relatively high thermal conductivity [7], inertness to hot and cold mineral acids and alkali solutions [8], favourable piezoelectric properties and high acoustic velocity [9], and high oxidation resistance in air [10]. The parabolic rate constants for oxidation of AlN in air follows Al_2O_3-forming kinetics. Rate constants are similar to alumina-forming kinetics of NiAl for temperatures ranging to 1100 °C [10]. Alumina scales are excellent barriers to penetration by oxygen and grow at a slower rate than silica scales at temperatures to about 1300 °C [11].

Advantages of aluminium nitride over alumina as a matrix material for silicon carbide-reinforced composites include (a) weight savings due to a 15% lower density, and (b) greater compatibility with silicon carbide. Aluminium nitride-silicon carbide solid solutions have received considerable attention in recent

0022–2461

years. Aluminium nitride exists in a hexagonal (wurtzite) crystal structure (2H) with strong covalent bonds. Silicon carbide is also a covalent compound which exists either in a cubic structure (β – SiC, 3C) or in various hexagonal or rhombohedral polytypes (α–SiC, e.g. 2H, 4H, 6H, 15R, and 21R). The lattice parameters of 2H SiC are fairly close to those of aluminium nitride; the theoretical densities and the molecular weight are nearly the same. To date, aluminium nitride/silicon carbide ceramics have been prepared mainly by hot pressing of powders [12–17]. A wide range of compositions have been hot pressed to high density. A flexural strength of up to 1 GPa was achieved in AlN–SiC materials and was attributed to a dense, equiaxial grain structure of the 2H(δ) AlN–SiC solid solution, with a relatively uniform grain size of $\sim 1\,\mu m$ [18]. The strength was found to decrease with increasing grain size. Little, if any, work has been done in regard to reinforcing aluminium nitride matrix with silicon carbide whiskers.

2. Experimental procedure

2.1. Fabrication of billets

2.1.1. Raw materials

The raw materials utilized in the composite blend were Advanced Refractory Technologies, Inc., grade A-100 aluminium nitride, Advanced Composite Materials Corporation grade SC-9 silicon carbide whiskers, and Molycorp, Inc., Code no. 5600 yttrium oxide. A 40 kg composite powder blend with the composition of 68 wt % AlN, 30 wt % SiC_w, and 2 wt % Y_2O_3, was purchased from Advanced Refractory Technologies. Advanced Composites Materials performed the blending process via a ball-milling technique that was considered proprietary.

Scanning electron micrographs of the composite blend (Fig. 1) showed a well-mixed blend of whiskers and powders. The powder particles were in the 1–5 μm size range and the whiskers were of the order of 0.5 μm diameter. However, the range of whisker lengths appeared to have been reduced in the mixing process from 10–80 μm to 5–30 μm.

The monolithic aluminium nitride specimens were made according to a pressureless sintering technique at Keramont Corporation. They have developed a proprietary process for producing this material with very high thermal conductivity.

2.1.2. Hot pressing

Consolidation of the composite powder blend was achieved by hot uniaxial pressing at Babcock and Wilcox. Hot pressing was performed in a 200 ton, single-action press using induction heating. An initial 1.5 h burn-out step, consisting of heating at low power below red heat while evacuating, was added to the hot-pressing cycle after a weight-loss problem was diagnosed. After the burn-out step, the dies were heated at full power under a flowing nitrogen atmosphere while pressure was applied gradually as the die temperature increased to the soak range of 1500–1700 °C. Temperature was measured using an optical pyrometer which was sighted on the top surface of the die sleeve. Actual powder blend temperature was probably considerably higher. A typical hot-press cycle time–temperature–pressure profile is shown in Fig. 2. Densification was monitored by measuring the travel of the top ram with a dial gauge, and when it slowed to a negligible rate of movement (5×10^{-4} cm min^{-1}) the cycle was ended.

After hot pressing, the die sleeves were cut open in order to remove the hot-pressed composite billets. The

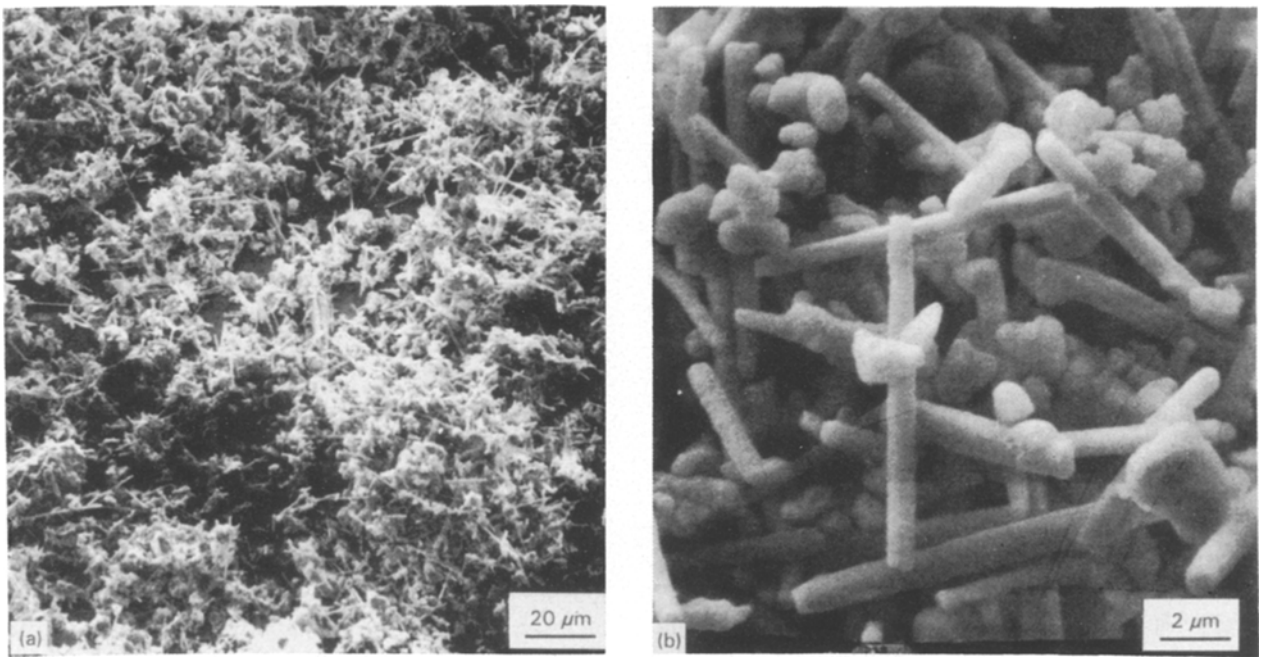

Figure 1 Photomicrographs of the as-received SiC_w/AlN composite powder blend.

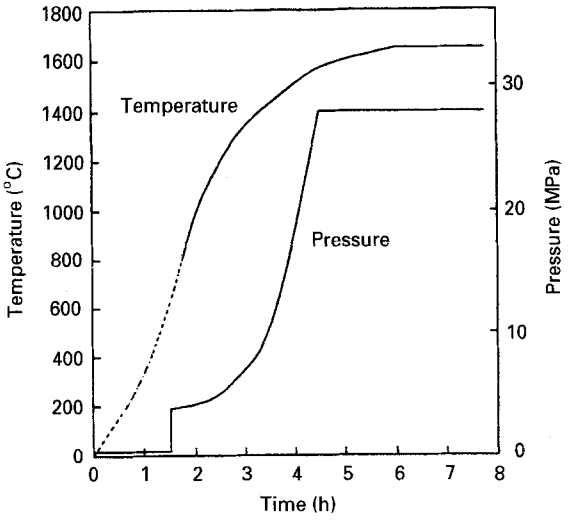

Figure 2 Time–temperature–pressure profile of hot-press cycle 1117.

billets were cleaned up by belt sanding and surface grinding prior to measuring their bulk densities. Immersion bulk densities were determined by dividing the billet dry weight by the result of subtracting the weight when immersed in water from the dry weight.

A total of seven 25 cm (10 in) composite billets were hot pressed. Five of the billets were $\geqslant 98\%$ calculated theoretical density of 3.27 g cm^{-3}. Test coupons were fabricated from the 25 cm diameter composite billets.

2.2. Test set-up

Because an ASTM procedure for flexural testing of structural ceramics does not exist, MTL-TT-87-35 was used as a guide. Flexural strength was measured on several specimens from each billet. Test bars measured 76 mm × 6.1 mm × 3.0 mm (3 in × 0.24 in × 0.12 in) were taken from various billet locations. Longitudinal finishing grinds were made on the bars using a 320 grit diamond wheel. Edges were bevelled with a diamond hone. The four-point bend tests were conducted at ambient conditions using an inner span length of 22 mm (0.875 in), an outer span of 67 mm (2.625 in), and a cross-head speed of 0.51 mm min^{-1} (0.02 in min^{-1}) in an MTS testing machine. The tensile axis of the bars was perpendicular to the hot pressing direction while the tensile surface was parallel to it. Young's modulus was determined from the stress–strain curves obtained from the load versus deflection plots.

Tensile and fatigue test coupons were machined according to the configuration shown in Fig. 3a. Owing to the extremely brittle nature of the material, it was necessary for a special gripping arrangement. This gripping technique (Fig. 3b) generally provided valid

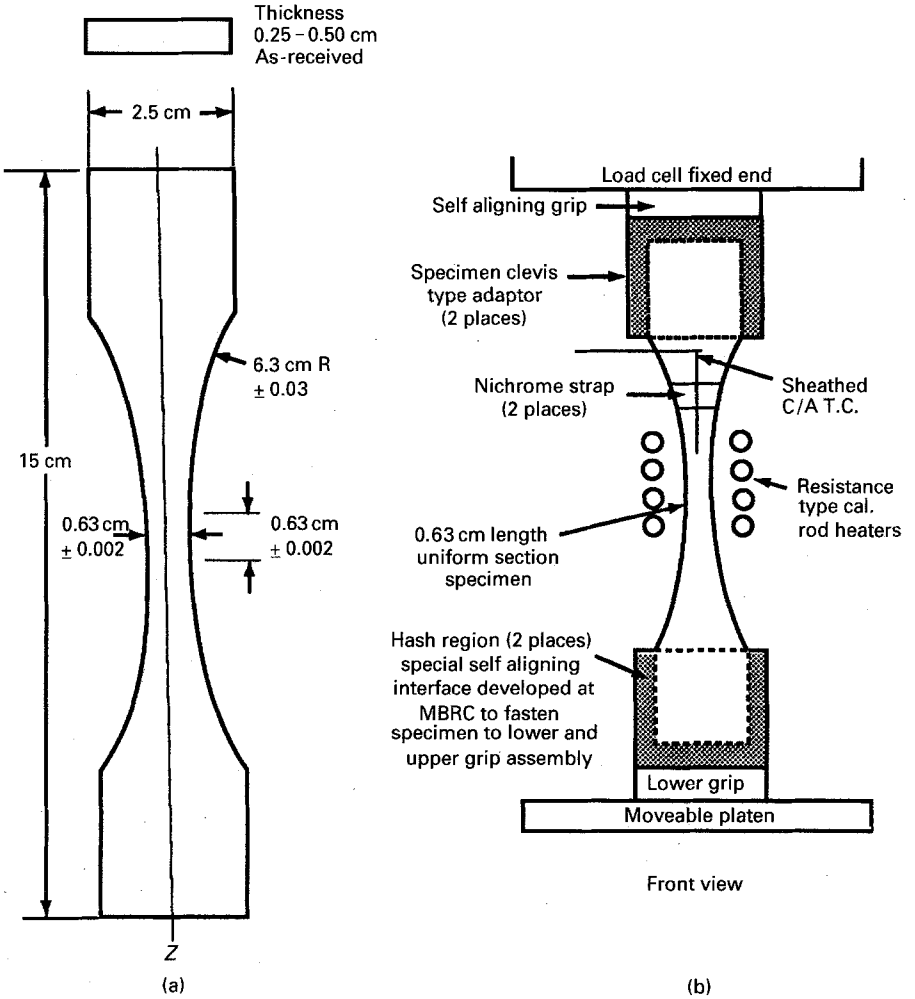

Figure 3 Sketch describing tensile and high-cycle fatigue test set-up; (a) specimen configuration, and (b) test fixture.

results and only a few tests were lost due to alignment and gripping limitations.

3. Results

3.1. Flexure tests

Results of the flexure tests for both AlN and SiC_w/AlN coupons are shown in Table I. Young's modulus values are also shown in the table. Flexure test results for the composite are values obtained from four different billets. Specimen bulk densities for the SiC_w/AlN composite, shown in Table I, were greater than 98% theoretical density in all cases. The flexural strengths of the SiC_w/AlN coupons from all four billets were relatively high and quite consistent, between 400 and 500 MPa. These values were considerably higher than obtained for the monolithic AlN (~255 MPa). Young's modulus values for the whisker-reinforced composite were similar to those for AlN, on the order of 300 GPa, for the higher density specimens and were lower, as expected, for the higher porosity coupons. Modulus values obtained for the monolithic AlN (~283 GPa) are in excellent agreement with previously reported values of ~ 275 GPa [16, 19].

The fracture origin areas of most of the test specimens were located adjacent to the tensile surface (Fig. 4). However, close examination of the apparent origin regions in four of the specimens by SEM did not reveal any obvious flaws or defects at the fracture origin sites. The fracture surfaces were quite rough in general (Fig. 5). Crack routing around whiskers, whisker protrusions, and whisker-shaped cavities were evidence of possible toughening by crack deflection and pullout mechanisms.

TABLE I Flexural strength data for AlN and SiC_w/AlN

Material	Specimen bulk density ($g\,cm^{-3}$)	Four-point flexural strength (MPa)	(10^3 p.s.i.)	Young's modulus (GPa)	(10^6 p.s.i.)
AlN	–	269	39	276	40
	–	248	36	269	39
	–	276	40	283	41
	–	235	34	290	42
	–	269	39	297	43
	–	221	32	290	42
Average	–	255	37	283	41
SiC_w/AlN (Billet no. 1111)	3.19	480	70	250	36
	3.22	490	71	280	41
	3.12	410	59	210	30
Average	3.18	460	67	250	36
(Billet no. 1112)	3.25	460	66	320	46
	3.25	460	67	300	43
	3.22	480	70	290	42
Average	3.24	470	68	300	44
(Billet No. 1115)	3.23	490	71	300	43
	3.25	410	60	300	43
	3.23	460	71	300	44
Average	3.24	490	67	300	43
(Billet no. 1117)	3.25	410	60	300	43
	3.27	490	71	310	45
	3.25	480	70	310	45
Average	3.26	460	67	310	44

3.2. Tensile tests

The tensile test results for both AlN and SiC_w/AlN coupons are shown in Table II. Ultimate tensile strengths for the reinforced material (~275 MPa) were approximately double that of the monolithic AlN (~ 125 MPa). Young's modulus values obtained

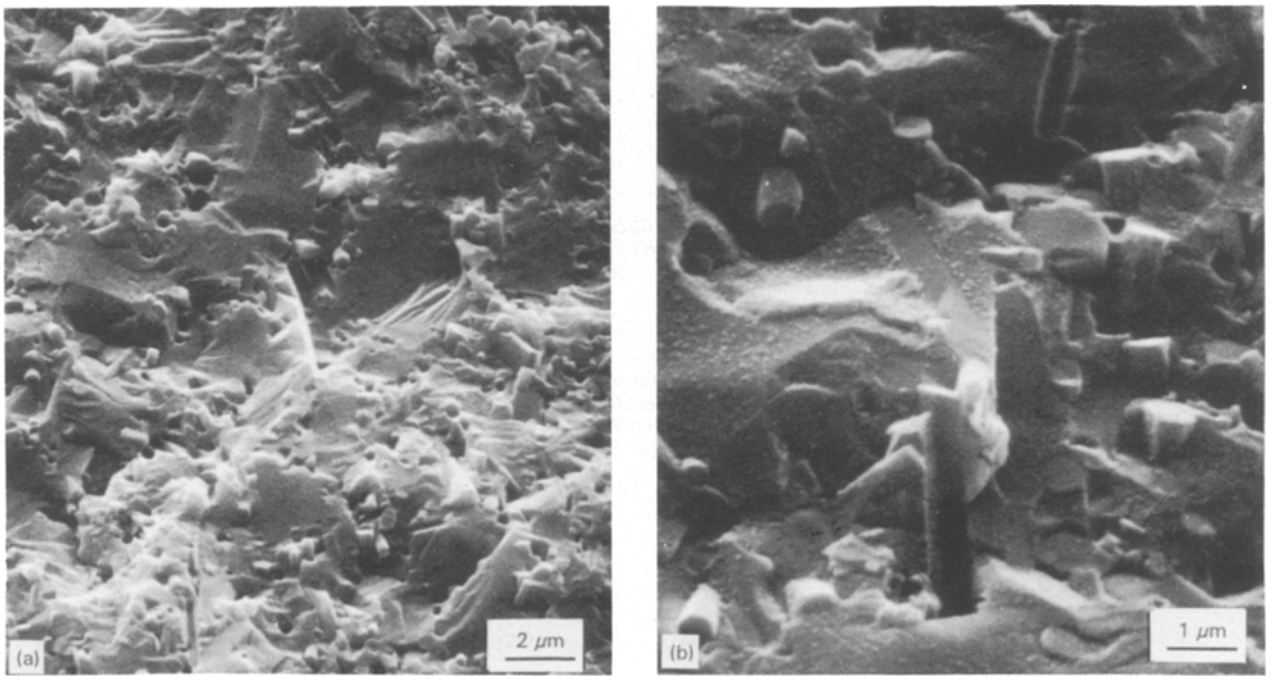

Figure 4 Fracture origin region in SiC_w/AlN composite flexural strength test specimen 1112-20-A.

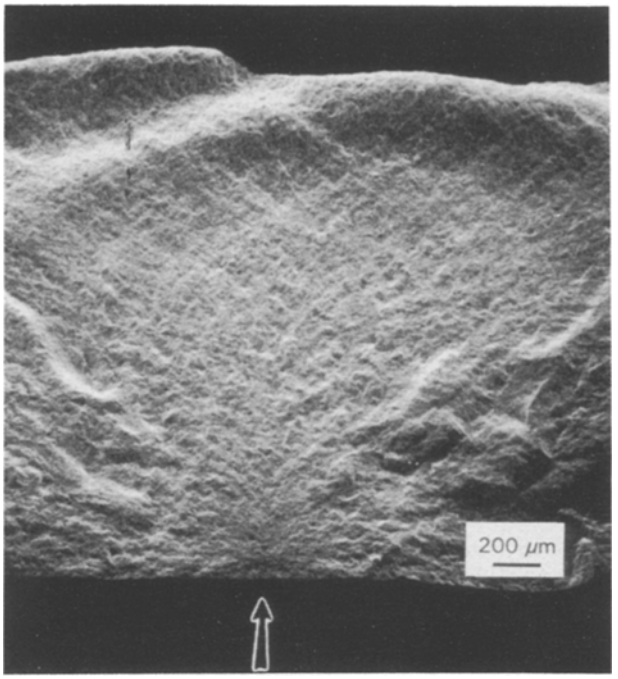

Figure 5 Fracture surfaces of SiC_w/AlN composite specimen 1112-20-A showing evidence of crack deflection and whisker protrusions and cavities (submicrometre nodules are artefacts from sample preparation sputtering).

TABLE II Tensile strength data for AlN and SiC_w/AlN

Material	Ultimate strength (MPa)	(10^3 p.s.i)	Modulus of elasticity (GPa)	(10^6 p.s.i.)	Strain-to-failure (%)
AlN	122.1	17.7	306.3	44.4	0.04
	131.1	19.0	307.7	44.6	0.04
	118.7	17.2	309.1	44.8	0.04
	106.3	15.4	316.0	45.8	0.05
	149.0	21.6	320.2	46.4	0.04
Mean	125.4	18.2	311.9	45.2	0.04
SiC_w/AlN	258.1	37.4	314.6	45.6	0.09
	269.1	39.0	218.0	31.6[a]	0.14
	248.4	36.0	310.5	45.0	0.08
	298.1	43.2	306.4	44.4	0.10
	304.3	44.1	292.6	42.4	0.10
Mean	275.6	39.9	306.0	44.4	0.10

[a] Omitted for calculating mean.

from tensile tests were fairly similar for the reinforced and unreinforced material. As shown in Table II, the total strain to failure for the monolithic materials was 0.04%. The reinforced material exhibited approximately 0.1% strain at the failure point. This value is at least a factor of 2 improvement over the monolithic material.

3.3. High-cycle fatigue tests

The fatigue test results are presented for both reinforced and unreinforced material in Table III. Plots of maximum stress versus cycles-to-failure for the materials evaluated are shown in Fig. 6. In some cases, stress levels greater than those obtained in the tensile test

TABLE III High-cycle fatigue results for SiC_w/AlN and AlN (room temperatures, $R = 0.1$, freq. = 20 Hz, load control)

Coupon type	Maximum stress (MPa)	(10^3 p.s.i.)	Cycles-to-failure, (N_f)
AlN	207	30	1235
	179	26	187 567
	172	25	1588
	172	25	739 672
	172	25	1000
	166	24	5546 584
	164	23.8	316
	163	23.7	1071
	162	23.5	30 783 684
	152	22	87 737 258
	145	21	1889 000
	138	20	3500 000
	127	18.4	1000
	110	15.9	1300
	104	15	> 10 000 000
	90	13	> 10 000 000
	76	11	> 10 000 000
SiC_w/AlN	373	54	405 580
	352	51	2627 296
	345	50	12 397 051
	345	50	10 029 700
	338	49	876 820
	331	48	2996
	324	47	> 10 405 900
	324	47	100
	321	46.5	64 398
	317	46	28 406 414
	317	46	64 239
	311	45	5517 778
	297	43	> 10 000 000
	290	42	> 11 575 750

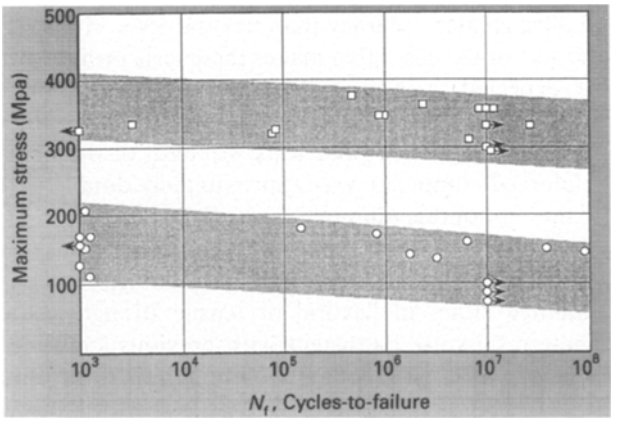

Figure 6 High-cycle fatigue data for AlN and SiC_w/AlN composites ($T = 25\,°C$, freq. = 20 Hz, load control). (○) AlN, (□) SiC_w/AlN.

results were employed in the high-cycle fatigue portion of the programme. As shown in Fig. 6, the SiC_w/AlN coupons subjected to stress levels of 310 MPa or less yielded cyclic lives of greater than 10^6 cycles. These stress levels are higher than the monolithic tensile strengths obtained for this material (275 MPa). Also, a similar result was observed for the monolithic material. Stress levels of 207 and 179 MPa yielded fatigue lives of approximately 1300 and 190 000 cycles, respectively. These stress levels are

considerably greater than the ultimate tensile strength obtained for the material. Obviously, these materials both have the ability to sustain higher stress levels in the cyclic tests as compared to the tensile test results.

4. Discussion

The flexural strength measured in the SiC_w/AlN composite (460 MPa) is close to that previously measured in alumina – 20 vol % SiC specimens containing similar-type SiC whiskers. In those studies, a flexural strength of 445 MPa was obtained in reinforced alumina composites containing SiC fibres of diameter 0.3–0.4 μm [20]. Larger flexural strengths and fracture toughnesses were obtained for the same composition when SiC fibres of diameter 1.5–2.5 μm were used. The improvement in mechanical properties with increase in fibre diameter was explained in terms of residual stress effects. Small-diameter whiskers have the tendency to form whisker bundles and, consequently, to increase residual stress concentration in the matrix as a result of stress field superposition [20].

The flexural strengths measured in the SiC_w/AlN coupons were also similar to that measured in an aluminium nitride/silicon carbide composition (70 AlN – 30 SiC/mol %) prepared by hot pressing [21]. In those studies, a flexural strength of 450 MPa was obtained for material of 5–6 μm grain size. Small grain size is considered important in achieving high strength in AlN–SiC solid solutions. Flexural strengths of 1 GPa were obtained for a 75 SiC–25 AlN (mol %) composition which contained a dense, equiaxed grain structure of grain size ~1 μm [21].

Tensile strength data on ceramic materials are limited. The tensile strength tests are normally expected to offer greater accuracy than flexural tests. However, the additional cost often makes these tests prohibitive. As expected, measured flexural strengths for both SiC_w/AlN and AlN were considerably greater than tensile strengths. In both tests, strength of the fibre-reinforced composite was approximately double that of the monolithic aluminium nitride.

Additions of 30 wt % SiC in the form of whiskers were found to have little effect on modulus readings obtained either in flexural or tensile strength data. These results are consistent with previous studies of sintered AlN–SiC composites containing 20 and 30 vol % SiC, respectively, which showed little or no increase in Young's modulus [16, 22]. Measured values of Young's modulus for hot-pressed SiC (~440 MPa) are somewhat higher than values measured in AlN. The elastic properties of a unidirectional fibre composite containing fibres is a function of the elastic properties of fibres and matrix and of their relative volumes in the composite material. For randomly reinforced whiskers, the analysis is much more complex, however.

High-cycle tensile fatigue results for SiC_w/AlN coupons at room temperature were also considerably improved over monolithic AlN. Maximum tensile stresses producing equivalent fatigue life were approximately in the ratio of 2:1 for the whisker-reinforced material compared to the pressureless AlN. High-cycle tensile fatigue results in SiC_w/AlN coupons are comparable to previous results obtained in C/SiC composites [22]. In those tests, 0°, 190° C/SiC coupons were tested at room temperature in tension-tension with $R = 0.1$, and a frequency of 50 Hz. Based on the samples tested, the fatigue limit was approximately 317 MPa. This value is almost identical to values obtained for SiC_w/AlN coupons at ambient temperature. Scatter in experimental data was also very similar in the different experiments.

The larger stresses sustained by AlN and SiC_w/AlN cyclic tests compared to static tensile tests may be due to the amount of time that the specimens were exposed under a given stress for the two different types of tests. This behaviour suggests that a strain-rate sensitivity exists for these types of materials. For the cyclic tests conducted at a 20 Hz frequency, the peak stress is applied to the specimen for a time period approaching 0.5 ms. The tensile tests were conducted at a strain rate of 0.5% min^{-1}. With consideration for an equivalent stress of 373 MPa, the time at peak stress would equal approximately 2 s. This value is approximately 4000 times longer than the time under an equivalent stress in a fatigue cycle operating at the 20 Hz frequency. This behaviour may be due to the extreme notch sensitivity exhibited by the material being evaluated. The longer period of time under an applied stress would allow local stress concentrations due to a self strengthening or seating type of realignment to become more significant.

5. Conclusions

1. Billets of an SiC_w/AlN composite blend, 25 cm (10 in) diameter, were hot pressed to near theoretical density. The maximum density was attained at the peak processing parameters of 1700 °C die temperature and 28 MPa (4000 p.s.i.) pressure.

2. SiC_w/AlN composites consisting of 30 wt % SiC_w produced a large increase in flexural strength, tensile strength, and tensile fatigue strength compared to monolithic AlN. Increases were nearly double in all cases. Corresponding strain-to-failures measured in tensile tests increased from ~0.04% in monolithic AlN to ~0.10% in the SiC_w reinforced composite. Fracture surfaces showed evidence of whisker-toughening mechanisms due to additions of SiC_w whiskers.

3. High-cycle fatigue tests indicated that both AlN and SiC_w/AlN have the ability to sustain higher stress levels in the cyclic tests compared to the tensile experiments. The improved performance under cyclic testing is explained in terms of strain-rate effects. The times at or near peak stress are considerably less under high-cycle fatigue testing compared to tensile tests.

Acknowledgement

The authors thank K. W. Hill and H. H. Moeller, Babcock and Wilcox, for consolidation of the composite billets and helpful discussions. The authors are grateful to Dr W. R. Garver for supporting this effort.

References

1. P. F. BECHER, C. H. HSUEH, P. ANGELINI and T.N. TIEGS, *J. Am. Ceram. Soc.* **71** (1988) 1050.
2. P. F. BECHER and G. C. WEI, *ibid.* **67** (1984) C-267.
3. P. F. BECHER and T. N. TIEGS, in "Engineered Materials Handbook", Vol. 1," "Composites," (ASM International, Metals Park, OH, 1987) pp. 941.
4. P. F. BECHER, T. N. TIEGS and P. ANGELINI, "Fiber Reinforced Ceramics," edited by K. S. Mazdiyasni (Noyes, Park Ridge, NJ) in press.
5. P. ANGELINI, W. MADER and P. F. BECHER, in, "MRS Proceedings: Advanced Structural Ceramics," Vol. 78, edited by P. F. Becher, M. V. Swain and S. Somiya (Materials Research Society, Pittsburgh, PA, 1987) p. 241.
6. P. F. BECHER and T. N. TIEGS, *Adv. Ceram. Mater.* **3** (1988) 148.
7. G. A. SLACK, "Aluminium Nitride Crystal Growth, Final Report on Contract F49620-78-C-0021," Directorate of Electronic and Solid State Sciences, Bolling AFB, DC (December 1979).
8. J. A. KOHN P. G. COLTEN, and R. A. POTTER, *Am. Mineral.* **41** (1956) 355.
9. C. O. DUGGER, "The Single Crystal Synthesis and Some Properties of Aluminium Nitride", AF CRL-TR-75-0486, Air Force Cambridge Research Laboratories (August 1975).
10. C. K. UNNI, General Dynamics IR&D, unpublished data (1990).
11. F. S. PETTIT, *Trans. AIME* **239** (1967) 1296.
12. R. RUH and A. ZANGVIL, *J. Am. Ceram. Soc.* **65** (1982) 260.
13. S. Y. KUO, A. V. VIRKAR and W. RAFANIELLO, *ibid.* **70** (1987) C-125.
14. W. RAFANIELLO, M. R. PLICHTA and A. V. VIRKAR, *ibid.* **66** (1983) 272.
15. L. D. BENTSON and D. P. H. HASSELMAN, *ibid.* **66** (1983) C-40.
16. W. RAFANIELLO, K. CHO and A. V. VIRKAR, *J. Mater. Sci.* **16** (1981) 3479.
17. R. RUH, *Am. Ceram. Soc. Bull.* **64** (1985) 1368.
18. M. LANDON and F. THEVENOT, *Ceram. Int.* **17** (1991) 97.
19. K. KOMEYA and F. NODA, *Toshiba Rev.* **92** (1974) 13.
20. A. V. KRYLOV, S. M. BARINOV, D. A. IVANOV, N. A. MINDLINA, L. PARILAK, J. DUSZA, F. LOFAJ and E. RUDNARPEVA, *J. Mater. Sci.* **12** (1993) 904.
21. Y. XU, A. ZANGVIL, M. LANDON and F. THEVENOT, *J. Am. Ceram. Soc.* **75** (1992) 325.
22. Y. YAMADA, A. KAWASAKI, J. LI, M. TAYA, and R. WATANOBE, *J. Jpn Inst. Metals* **56** (1992) 1078.
23. DuPont Corporation, unpublished data.

Received 9 May
and accepted 22 July 1994